

## IV. SOLID-STATE MICROWAVE ELECTRONICS\*

### Academic and Research Staff

Prof. R. P. Rafuse  
Dr. D. H. Steinbrecher

### Graduate Students

W. G. Bartholomay  
A. Y. Chen  
R. D. Mohlere

D. F. Peterson  
J. E. Rudzki  
A. A. M. Saleh

R. W. Smith  
R. E. Snyder  
J. G. Webb

#### A. 60-GHz MIXER

The mixer has been assembled and tested. Using a 5-dB noise figure intermediate-frequency amplifier at 3.1 GHz, we have measured an over-all receiver noise figure of 12.2 dB. This corresponds to a 7.2-dB conversion loss mixer at 60.8 GHz.

The diodes used were gold gallium arsenide Schottky barrier diodes with a contact area of 5  $\mu\text{m}$ . The diodes were self-biased with a DC current slightly in excess of 10 mA each.

J. E. Rudzki

#### B. 15-GHz DOUBLER

With a new coupling pin designed by Dr. J. W. Majer, the input impedance measurements of a few diodes have been studied at 15.2 GHz. A waveguide tuner is now being designed for the input port of the doubler. More theoretical aspects of the doubler are also being investigated.

A. Y. Chen

#### C. AVALANCHE DIODE ANALYSIS

##### 1. Oscillator Analysis

The variation in output power and noise of the fundamental of an avalanche diode oscillator has been investigated as a function of higher harmonic (the second and third, for the most part) tuning. This was accomplished by mounting the diode in a special circuit that provided reasonable isolation of the fundamental from the higher harmonics, as shown in Fig. IV-1.

Tuning and coupling at the fundamental ( $\sim 9$  GHz) was provided by two movable copper slugs and an external double stub tuner (if necessary), while the tuning at the second (and third) harmonics was done by using a K-band adjustable waveguide backshort. The

---

\*This work was supported by the National Aeronautics and Space Administration (Grant NGL-22-009-163); and in part by the Joint Services Electronics Programs (U.S. Army, U.S. Navy, and U.S. Air Force) under Contract DA 28-043-AMC-02536(E).

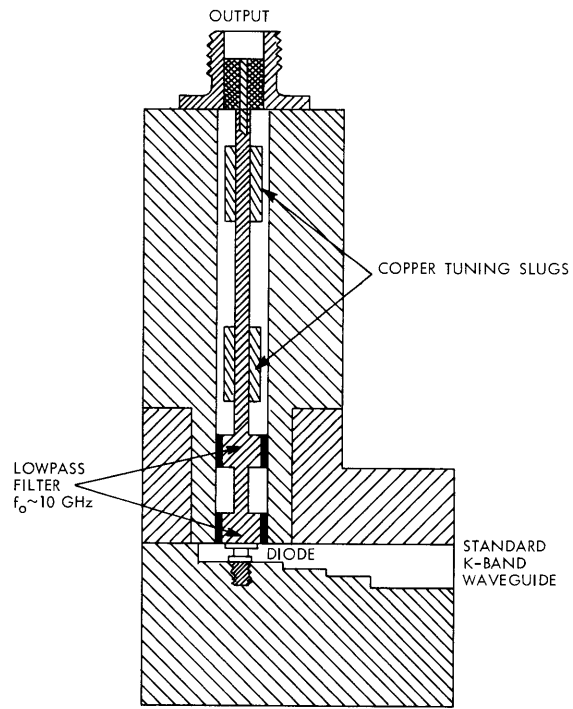


Fig. IV-1. An imbedding network providing the necessary coupling and tuning for the fundamental.

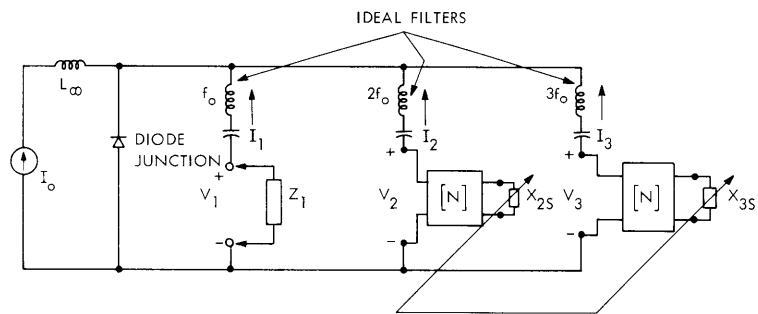


Fig. IV-2. Equivalent circuit.

#### (IV. SOLID-STATE MICROWAVE ELECTRONICS)

movable short provides the same type of impedance variation at  $3f_0$  as it does at  $2f_0$ ; that is,  $X_s = Z_w \tan \beta_3 L$ , since the reduced height waveguide at the diode forces the third harmonic to propagate in the  $TE_{30}$  mode.

The output power was observed to be a function of the tuning at both ports, and for fixed tuning at the fundamental a 2-3 dB variation in power level could be observed as the position of the adjustable short varied. The effect may be described in more quantitative fashion from consideration of the equivalent circuit (Fig. IV-2).

The tuning at the fundamental was described by the change in the real part of  $Z_1$ , and that at the 2nd and 3rd harmonics by the change in the position of the backshort relative to a given reference plane rp.  $X_{2S}$  and  $X_{3S}$  change together in some fashion, since each reactance is provided by the same adjustable short. The large series inductance of the cutoff waveguide essentially overwhelms any reactance change provided by the tuning slugs, thereby keeping the fundamental frequency nearly constant. Accordingly, this small variation in the reactive part of  $Z_1$  allowed the tuning at  $f_0$  to be characterized by its real part only. It should be mentioned that  $Z_1$  is the impedance seen by the junction at  $f_0$ , which can be found by the usual de-embedding procedure. The imbedding networks at  $2f_0$  and  $3f_0$  were not calculated in this experiment.

The procedure followed was to fix  $\text{Re} \{Z_1\}$  at several appropriate values and then observe the power-level variations as a function of the position of the backshort. In this manner a contour map of power output at the fundamental vs the tuning at each frequency involved was constructed. There are relatively high power plateaus at the smaller values of  $R_1$  ( $\text{Re} \{Z_1\}$ ), and its optimum value appears to be  $\sim 3.0 \Omega$  at 9.2 GHz. Both the second and third harmonics are of consequence, since peaks and valleys occur at half-guide wavelengths of these frequencies (although there is some ambiguity, since the guide wavelength at  $2f_0$  (0.970 in.) is nearly twice the guide wavelength at  $3f_0$  (0.496 in.).

Another consequence of the harmonic tuning was the variation it produced in the output noise, as seen on a spectrum analyzer. Figure IV-3 shows a typical power-level variation as a function of the position of the waveguide backshort. A rather profound variation in the noise performance was observed at each of the power-level droops. A sequence of photographs showing this effect is displayed in Fig. IV-4 where the letters below each picture correspond to the same letters in Fig. IV-3. Picture (f) represents the output with a matched load terminating the high-frequency port.

##### a. Incremental Avalanche Impedance Measurements

Incremental impedance measurements were made on an avalanche diode under non-oscillatory conditions to find its dependence on the direct avalanche current. The impedance was measured at some external reference plane using a slotted line or network analyzer, and then referred back to the diode junction through the appropriate coupling network. This coupling network was calculated from a knowledge of

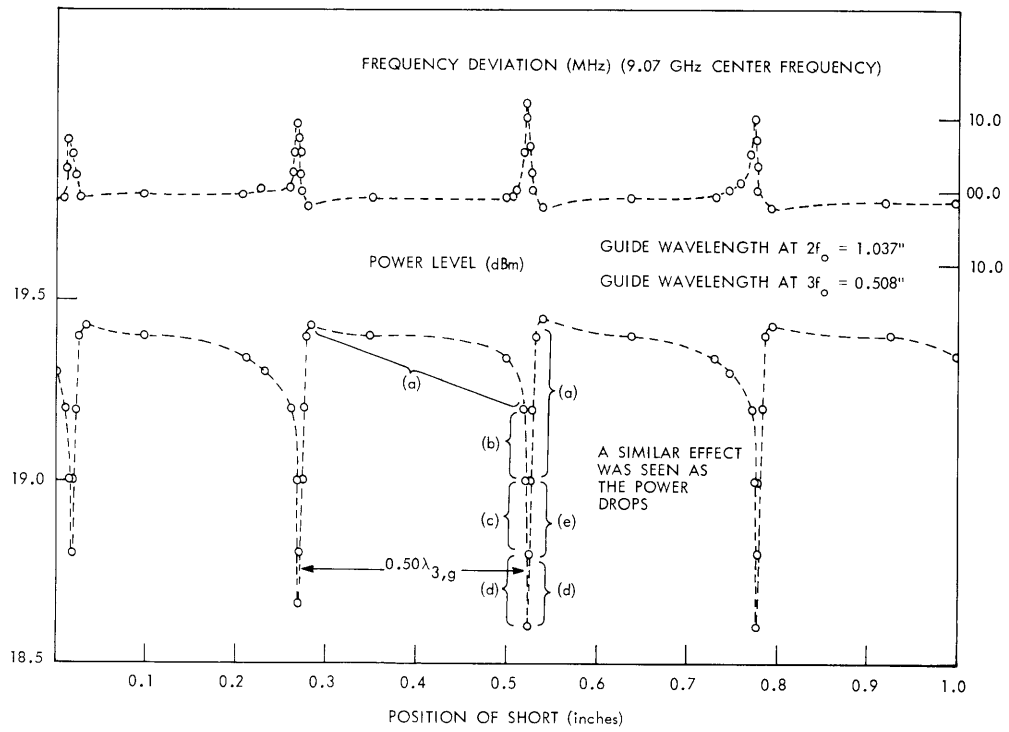


Fig. IV-3. Power and frequency deviation as a function of harmonic tuning. (Letters (a)-(e) refer to pictures in Fig. IV-4.)

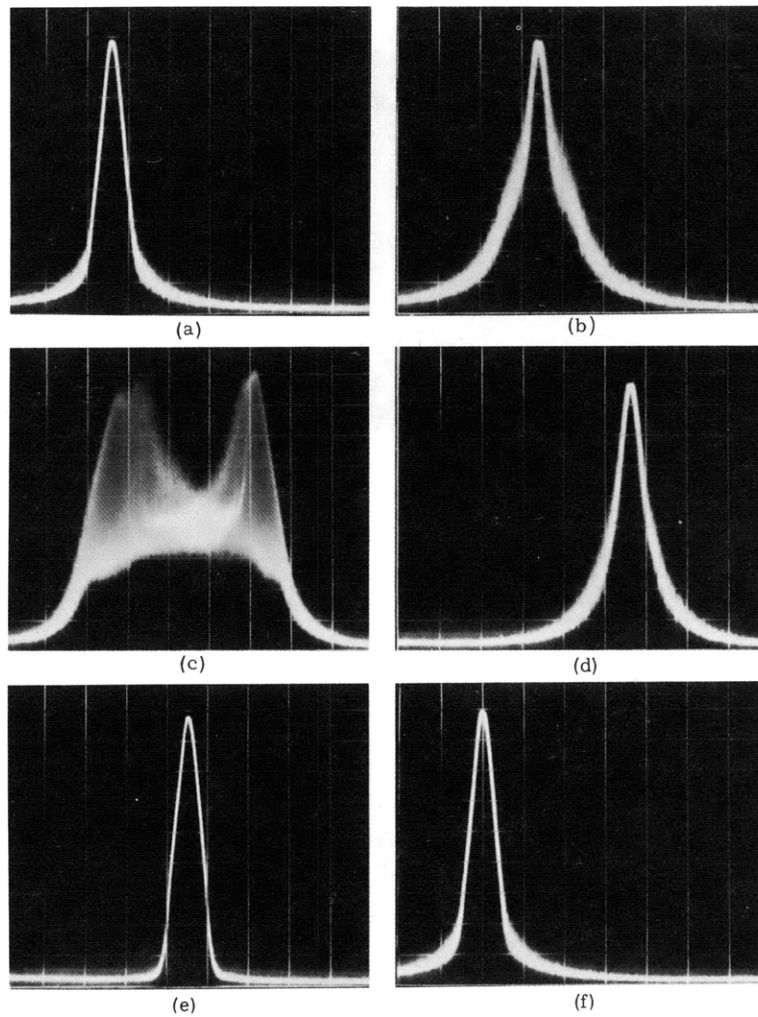


Fig. IV-4. Spectrum analyzer display of the fundamental output as a function of harmonic tuning. Letters correspond to the positions of the short as shown in Fig. IV-3. The pictures were taken using the LOG scale of the spectrum analyzer, with 1-MHz bandwidth and 15-MHz dispersion.

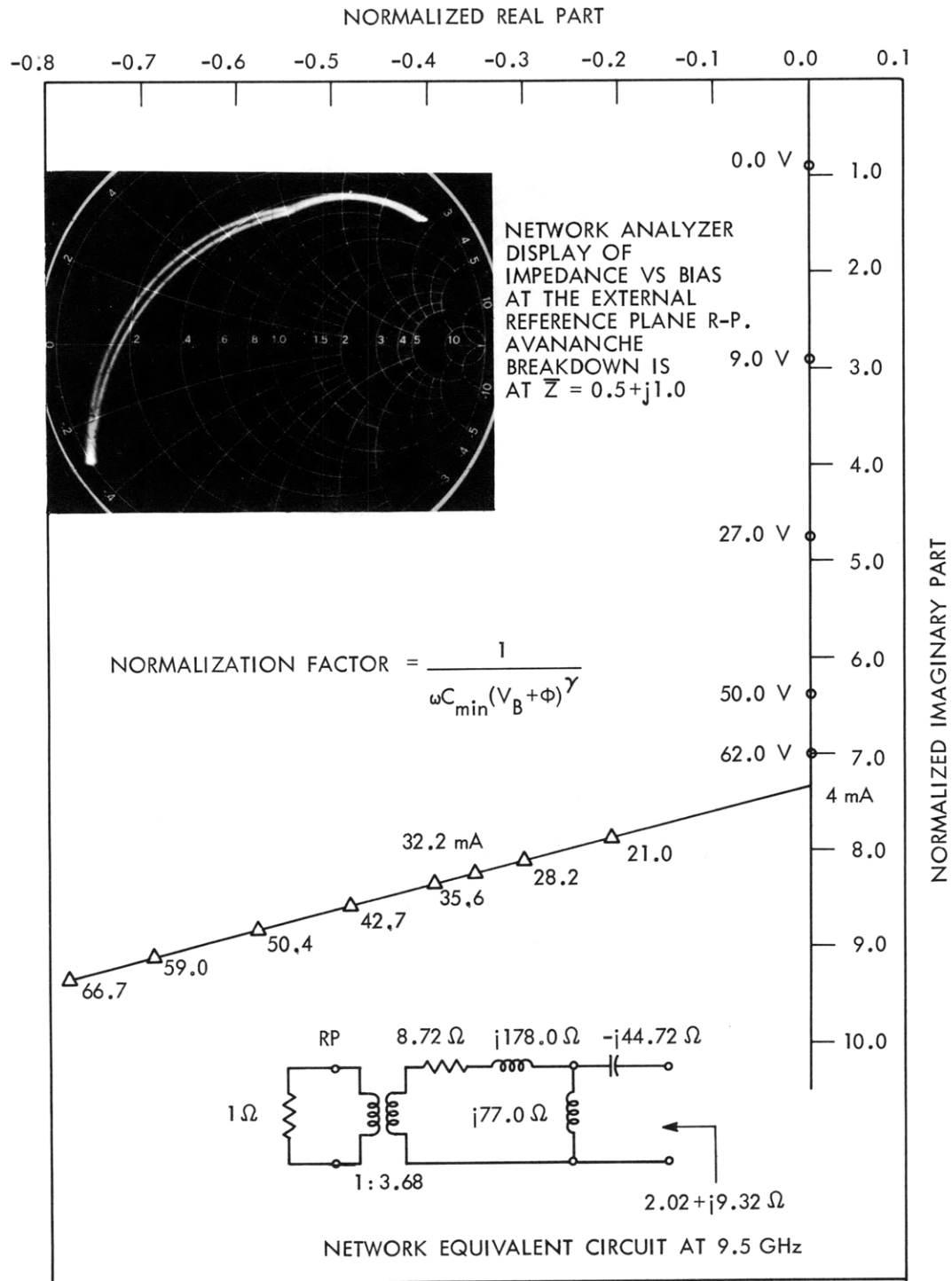


Fig. IV-5. Incremental diode impedance vs bias.

#### (IV. SOLID-STATE MICROWAVE ELECTRONICS)

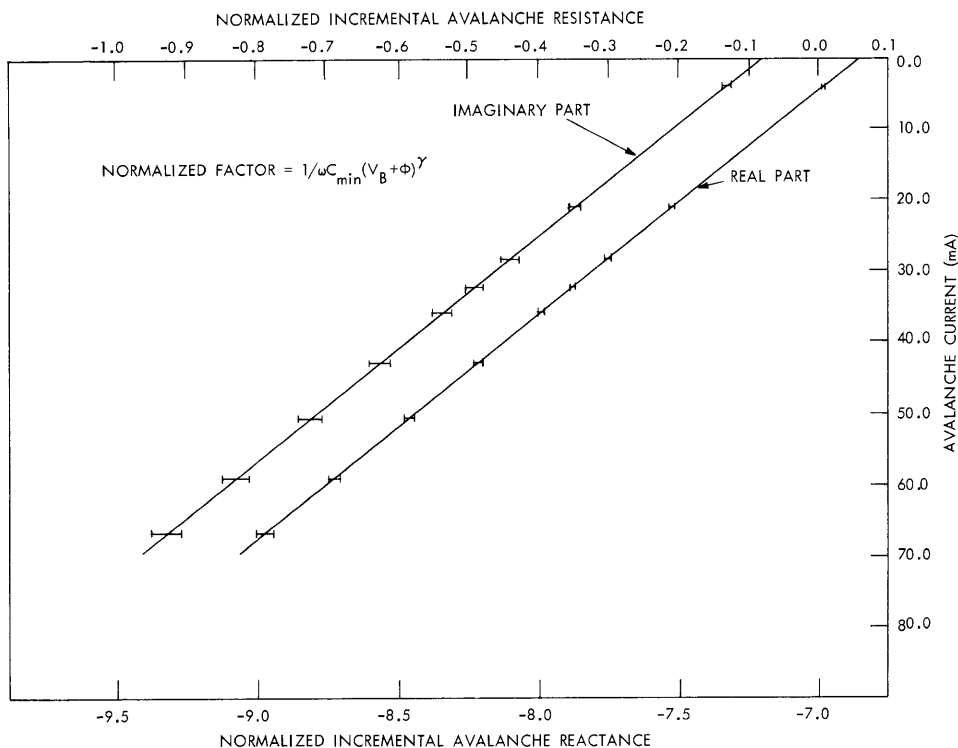


Fig. IV-6. Incremental diode impedance vs bias.

three impedance values at the junction and the corresponding values at the external reference plane. The three values of junction impedance used correspond to the reactance of the depletion layer capacitance at 3 specified bias voltages above avalanche breakdown.

Figure IV-5 shows the variation in impedance at the external reference plane (insert) and the corresponding variation at the junction after de-embedding. In the display (insert), the bias was swept at 60 Hz and avalanche breakdown is at the intersection of the two arcs (the hysteresis is due to heating effects). Figure IV-6 shows the variation of both real and imaginary parts of the diode's incremental impedance; it appears to be a linear function of the avalanche current at 9.5 GHz.

#### b. Negative R Amplifier

A Smith Chart plot of impedance vs bias at the output of the circuit of Fig. IV-1 indicates that for certain values of bias the real part is negative. The amount of negative resistance depends on the diode and the circuit losses, but it was large enough in this case to be used as a negative R amplifier. By attaching a 4-port circulator to the output, and adjusting the DC bias to maximize the magnitude of  $\Gamma$  without permitting self-oscillation of the avalanche diode, gain and bandwidth

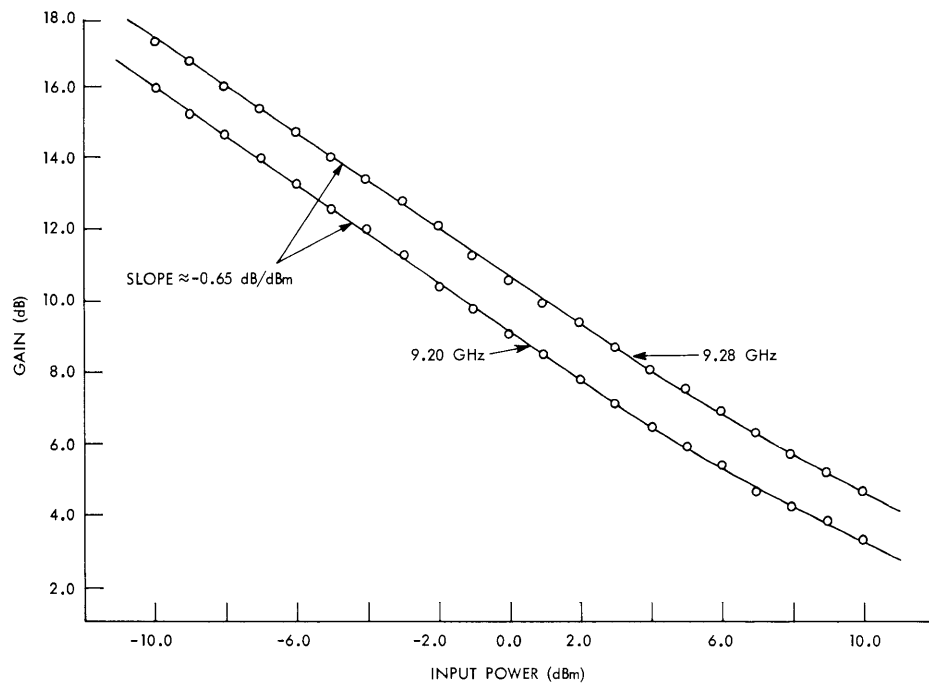


Fig. IV-7. Power gain vs input power with the avalanche diode used as a negative resistance amplifier.

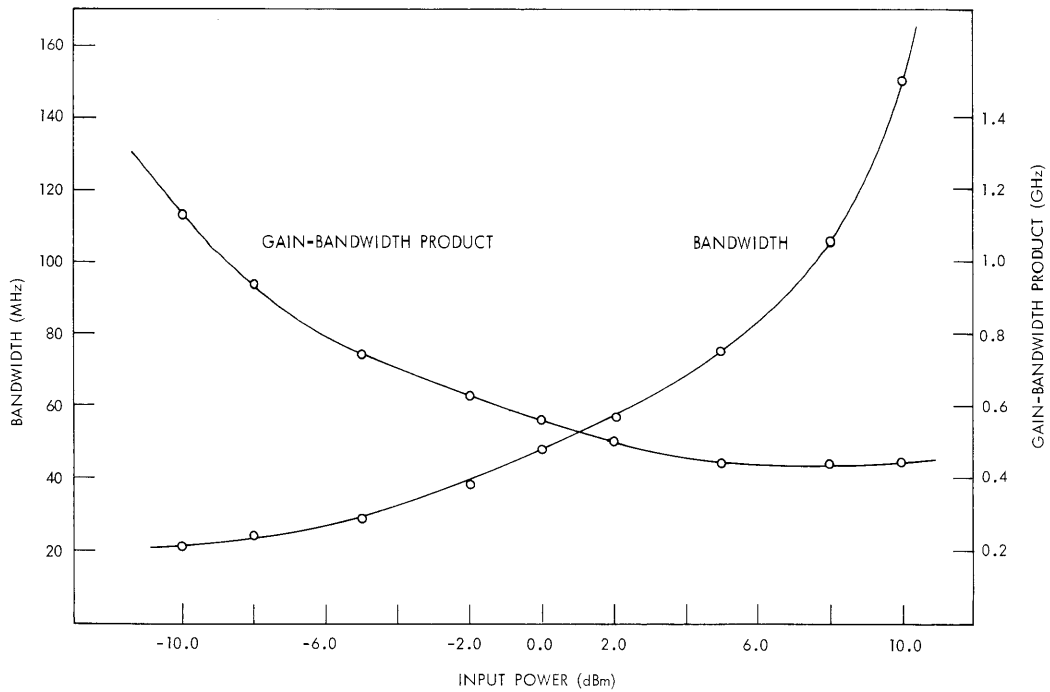


Fig. IV-8. Bandwidth and gain-bandwidth product for the avalanche diode negative resistance amplifier at 9.28 GHz.



#### (IV. SOLID-STATE MICROWAVE ELECTRONICS)

measurements were made as a function of the input power. Since the network contained a rather highly tuned circuit, the bandwidth is quite narrow. Figure IV-7 shows the power gain vs input power at two closely spaced frequencies for a Varian Associates avalanche diode. The curve has a nearly constant slope of  $-0.65$  dB/dBm. Figure IV-8 shows the bandwidth and gain-bandwidth product vs input power. The bandwidth might be stretched to 1 GHz with the proper circuit.

Noise-figure measurements on this amplifier ranged between 30 dB and 40 dB, which is typical for amplifier circuits employing avalanche diodes as the negative R device.

#### 2. Summary and Conclusions

The results of the oscillator analysis seem to clearly imply a consideration of harmonic terminations in the design of avalanche diode circuits. The noise performance and power output might be further improved by providing independent tuning at the second, third, and possibly higher harmonics. Noise-figure measurements using the avalanche diode as the local oscillator for an X-band balanced mixer have shown a 6-8 dB variation as the second harmonic was tuned with the adjustable backshort. This gives a sort of quantitative measure to the spectrum analyzer displays. Accordingly, a large-signal avalanche diode negative resistance amplifier might show noise-figure improvements with harmonic tuning.

The incremental avalanche impedance appears to have a nearly linear relation to the direct avalanche current. This implies some sort of nonlinear relation between the instantaneous voltage and current, which can be found from a knowledge of the frequency behavior of the incremental impedance. This brings up the possibility of using the avalanche diode as a self-pumped parametric amplifier, that is, letting the oscillator signal be the pump. A further use might be in the area of harmonic generators.

D. F. Peterson

